# Optimisation of DSF and SOA based Phase Conjugators by Incorporating Noise-Suppressing Fibre Gratings

Paper no: 1471

S. Y. Set, H. Geiger, R. I. Laming, M. J. Cole and L. Reekie

*Optoelectronics Research Centre*

*University of Southampton*

*Southampton SO17 1BJ*

*United Kingdom*

*Fax: +44 1703 593142* *Tel: +44 1703 593138*

*email: sys@orc.soton.ac.uk*

**Abstract**

We compare the performance of dispersion-shifted-fibre (DSF) and semiconductor-optical-amplifier (SOA) based phase conjugators for a 10 Gb/s non-return-to-zero system with respect to conversion efficiency, noise figure and distortion. Fibre gratings are used for signal extraction and amplified spontaneous emission (ASE) suppression, allowing closer wavelength spacing and reducing the conjugation noise figure by up to 12 dB. Despite the higher SOA conversion efficiency, both conjugators give similar noise figures with ASE suppression. However, the DSF based conjugator has the advantage of distortion tolerance at higher input power.

## I. INTRODUCTION

Optical phase conjugation has attracted much recent research attention due to its potential application for group-velocity-dispersion and self-phase-modulation compensation in mid-point spectral inversion (MPSI) systems, and also for coherent wavelength conversion in optical switching and routing. The two most promising optical phase conjugation techniques are four-wave mixing (FWM) in either dispersion-shifted fibre (DSF) [1], [2] or semiconductor optical amplifiers (SOA) [3], [4]. A DSF based conjugator requires phase matching close to its zero dispersion wavelength for efficient four-wave mixing [5]. This restricts its wavelength flexibility compared to an SOA based conjugator which offers a much wider conversion bandwidth. Furthermore, the low FWM conversion efficiency in passive DSF seems to make the SOA a preferred phase conjugating medium [3]. However, in a practical communication system, conjugation optical signal-to-noise ratio (SNR) is more important than conversion efficiency [6]. The noise at the conjugate wavelength is usually dominated by the amplified spontaneous emission (ASE) noise from the pump and signal. The reduction of this noise has been demonstrated in an SOA based conjugator (i) by bandpass filtering of the pump and/or signal waves before mixing [6], [7] and (ii) by the insertion of a notch filter at the conjugate wavelength before the conjugator [8].

In this letter, SOA and DSF based conjugators are compared by investigating the conversion efficiency, noise and eye opening in a 10 Gb/s non-return-to-zero (NRZ) externally-modulated system, using an identical filtering network. We report for the first time the use of fibre gratings for efficient ASE noise filtering and conjugate signal extraction. The performance enhancement using these noise-suppressing gratings is also investigated.

## II. EXPERIMENTS

The experimental setup is shown schematically in Figure 1. Two single-frequency tunable lasers were used as signal and pump sources. The signal source ($\lambda_S$ = 1537 nm) was externally modulated with a $2^{31}$–1 pseudo-random bit sequence (PRBS) at 10 Gb/s. The polarisation of the CW pump source ($\lambda_P$ = 1536 nm) and the modulated signal were aligned using two polarisation controllers before they were combined in a 3 dB coupler. At the output of the coupler, the pump power $P_P$ has a fixed value of -12.4 dBm whilst the signal power $P_{IN}$ was variable. They were then preamplified using a 1480-nm-pumped erbium-doped fibre amplifier (EDFA) to a saturated power of ~10 dBm before they were launched into the phase conjugator. An optional hole-burning grating was inserted before the conjugator, acting as a bandstop filter to suppress the ASE before the conjugation media. Figure 2(a) shows the deep spectral hole (suppression $\alpha_c$ < -40 dB) with 1.2 nm bandwidth at the conjugate wavelength ($\lambda_C$ = 1535 nm).

The phase conjugation media used in the experiment were either a GaInAsP SOA (Alcatel A 1901 SOA) or 13 km of DSF (Corning SMF/DS) with a zero dispersion wavelength $\lambda_0$ at 1535 nm. The experiment was designed to achieve efficient FWM in the DSF by phase-matching near $\lambda_0$[5] and frequency up-conversion was employed to favour the SOA [3]. The total power launched into the phase conjugating media was chosen below the stimulated Brillouin threshold of the DSF.

The conjugator output spectrum was monitored through a 10 dB coupler and the signal, conjugate and ASE power levels $P_S$, $P_C$ and $P_{ASE}$ were measured [Figure 2(b) and (c)]. When the hole burning grating was used, it was difficult to establish the true ASE level at the

conjugate wavelength due to the limited resolution bandwidth of the spectrum analyser. The ASE power was measured at the spectral trough away from the conjugate wavelength and thus was over-estimated in some cases.

The conjugated wave was extracted from the conjugator output by an apodised uniform fibre grating with 0.5 nm bandwidth centred at $\lambda_C$, used in combination with a circulator to suppress the pump and the signal waves by 30 dB and 40 dB respectively. The close wavelength separation of 1 nm was allowed by the sharp cut-off of this grating. The extracted conjugated signal was then amplified by a low-noise 980-nm-pumped EDFA. The out-of-band ASE was suppressed by an additional 1.2 nm bandwidth optical bandpass filter before the conjugated signal was detected with a 6.4 GHz bandwidth photo-detector. We examined the eye-diagram on a digital oscilloscope and measured the Q value of the received eye [9].

## III. RESULTS AND DISCUSSION

The key performance parameters of a phase conjugator, namely conversion efficiency, noise figure and signal distortion, can be computed from the measured optical spectra and eye diagrams. Data were only taken in the respective working range of each conjugator configuration where good eye-opening was observed.

### *A. Conversion efficiency*

The output conversion efficiency $\eta = P_C / P_S$ may be defined as the ratio of conjugate power and signal power at the output of the conjugator. The input conversion efficiency $\eta' = P_C / P_{IN}$, frequently used in other literature, is defined as the ratio of the output conjugate power and

the input signal power. The measured input and output conversion efficiencies are plotted in Figure 3 with and without the hole-burning grating for a range of input powers $P_{IN}$.

When the signal input power $P_{IN}$ approaches the pump power $P_P$, the saturation in the preamplifier gain $G_{Er}$ causes a reduction in the amplified pump $G_{Er} \times P_P$ launched into the conjugator. The measured conversion efficiency decreases since the output of a FWM process is proportional to $G_{Er}^3 \times P_{IN} \times P_P^2$ [5]. The sharper roll-off in the conversion efficiency of the SOA based conjugator is due to additional saturation in the SOA. The 0.6 dB insertion loss of the hole-burning grating degrades the conversion efficiency of the DSF based conjugator by ~2 dB, whereas the gain associated with the SOA overcomes this loss.

The conjugate power of the SOA is ~10 dB higher, as inferred from their input conversion efficiencies (Figure 3). Since the DSF has a loss of 4 dB, the output conversion efficiency of the SOA conjugator is only ~6 dB higher than the DSF based conjugator over their respective working range. As we will show in the next section, the output conversion efficiency is more useful in the derivation of conjugate noise figures.

### *B. Noise Performance*

Figure 4 shows the optical SNR of the conjugate wave, measured as the ratio of conjugate power $P_C$ to ASE power $P_{ASE}$ in a 0.05 nm bandwidth. Without the hole-burning grating filter, the SNR of the SOA based conjugator is ~6 dB higher than the DSF based conjugator. This agrees with the difference in output conversion efficiency between the two conjugators. However, when the hole-burning grating is used to filter out the ASE at the conjugate wavelength before conjugation, both conjugators give similar SNR. This is due to the fact that

although the DSF based conjugator has a lower conversion efficiency compared to the SOA based conjugator, it does not generate extra ASE noise.

The conjugation noise figure plotted in Figure 5 gives a corresponding picture. The conjugation noise figure is defined as $F^c = P_{ASE}/h\nu h\eta B + 1/\eta$, where $h$ is Planck's constant, $\nu$ is the optical frequency, $\eta$ is the input conversion efficiency and $P_{ASE}$ is the depolarised ASE power measured within the resolution bandwidth $B$. This definition is based on the conventional definition of amplifier noise figure [10], with the assumption of large preamplifier gain, signal-ASE-beat dominated noise, and small signal-conjugate wavelength separation ($\lambda_S \approx \lambda_C$).

The increase in noise figure with increasing input power is due to the decrease in input conversion efficiency (Figure 3). Without the hole-burning grating, the DSF based conjugator noise figure is 6 dB higher compared to the SOA based conjugator. The inclusion of the hole-burning grating reduces the experimental noise figures considerably, by up to 7 dB and up to 12 dB in the SOA and DSF based conjugator respectively. Despite the much lower conjugate power in the DSF based conjugator, both conjugators have similar noise figures approaching the preamplifier noise figure of 8 dB.

The overall conjugation noise figure may also be computed from individual component parameters by considering the ASE noise contribution at the conjugate wavelength. Assuming Poisson photon statistics, large preamplifier gain, small output conversion efficiency ($\eta << 1$) and negligible passband loss in the hole-burning grating, the noise figure of the SOA and DSF based conjugators were derived:

$$F_{SOA}^{c} = F_{Er} + \alpha_c \frac{F_{Er}}{\eta_{SOA}} + \frac{F_{SOA}}{\eta_{SOA} G_{Er}} \quad (1)$$

$$F_{DSF}^{c} = F_{Er} + \alpha_c \frac{F_{Er}}{\eta_{DSF}} \quad (2)$$

where $F^{c}_{SOA}$, $F^{c}_{DSF}$, $F_{SOA}$ and $F_{Er}$ are the noise figures of the SOA based conjugator, the DSF based conjugator, the SOA and the erbium preamplifier, respectively. $\alpha_c$ is the hole-burning grating suppression at the conjugation wavelength, $\eta_{SOA}$ and $\eta_{DSF}$ are the output conjugation conversion efficiencies of the SOA and DSF based conjugators respectively, and $G_{Er}$ is the gain of the erbium preamplifier. Theoretical noise figures based on Equation (1) and (2) are plotted in Figure 5. The theory shows good agreement with the measured data within the measurement error. In cases when a hole-burning grating was used, the experimental noise figures are larger than the theoretical noise figures due to the over-estimated ASE measurements as discussed in section II.

Equations (1) and (2) show that in both cases the conjugation noise figures are affected by the preamplifier noise figure $F_{Er}$. Without the hole-burning grating to suppress the ASE noise at the conjugate wavelength ($\alpha_c = 1$), the dominating term is the second term $F_{Er}/\eta$. The conjugation noise figure is then dependent on the conversion efficiency of the respective conjugator. However, when a hole-burning grating is inserted, it suppresses the second noise figure term by $\alpha_c$. With more than 40 dB suppression ($\alpha_c = 10^{-4}$), the second term is effectively eliminated. The DSF based conjugator is then limited by the preamplifier noise figure $F_{Er}$ = 8 dB, however, the SOA based conjugator suffers extra noise contributed from the SOA's ASE.

### *C. Signal Distortion*

The eye penalty is measured as the ratio of Q (in dB) of the back-to-back eye to that of the conjugated eye (Figure 6). The insertion of the hole-burning grating improves the sensitivity reduces the eye penalty of the SOA and DSF based conjugators by 5 dB and 10 dB respectively. Additionally, the minimum achievable eye penalty is improved by 1 dB for the SOA and by 3 dB for the DSF. Although both conjugators exhibit similar noise figures with the hole-burning grating, the eye penalty of the DSF based conjugator is ~1 dB worse than the SOA based conjugator at lower input powers. This is due to additional noise degradation caused by the post-amplification of the DSF's lower conjugate power. A low-noise postamplifier is thus essential for a DSF based conjugator.

At lower input powers, an increasing signal power causes increasing conjugate power and decreasing eye penalty, and the performance is limited by the conjugation noise figure. By increasing the input signal power to equal the pump power, $P_{IN} = P_P$, the eye penalty of the DSF based conjugator can be reduced to 0.8 dB. However, with increasing $P_{IN}$ , the eye penalty of the SOA based conjugator can only be reduced to 1.5 dB at $P_{IN}$ = -23 dBm. For increased signal powers, distortion sets in due to the inter-symbol-interference (ISI) caused by slow gain recovery in the SOA [6]. The optimum input signal power is approximately 12 dB below the pump power. Therefore, in the preferred working region, the DSF gives a better overall performance for its distortion tolerance.

## IV. CONCLUSION

We have compared the two most important optical phase conjugators for telecommunications with an innovative filter concept. The conjugation performance was significantly improved by inserting a hole-burning grating between the preamplifier and the conjugator to remove ASE at the conjugate wavelength and employing a narrow band conjugate signal extraction grating. We have derived conjugate noise figure equations for both conjugators based on individual component parameters which enable noise figure estimation in the design of a phase conjugator.

Although the SOA based conjugator offers a larger conversion efficiency, both conjugators give a similar conjugate noise figure using this noise filtering technique. However, a higher input power could be employed with the DSF based conjugator without distortion thus giving a superior performance.

## ACKNOWLEDGEMENT

The authors wish to thank Anritsu UK for the loan of the BER test equipment and Corning for the provision of the DSF. This work is funded in part by the European Union within ACTS project 'MIDAS'. The Optoelectronics Research Centre is an EPSRC-funded Interdisciplinary Research Centre.

## REFERENCES


[1] K. O. Hill, D. C. Johnson, B. S. Kawasaki, and R. I. MacDonald, "CW three-wave mixing in single-mode optical fibers," *J. Appl. Phys.*, vol. 49, pp. 5098–5106, 1978.

[2] S. Watanabe, T. Naito, and T. Chikama, "Compensation of chromatic dispersion in a single-mode fiber by optical phase conjugation," *IEEE Photon. Technol. Lett.*, vol. 5, pp. 92–95, 1993.

[3] S. Murata, A. Tomita, J. Shimizu, and A. Suzuki, "THz optical-frequency conversion of 1 Gb/s-signal using highly nondegenerate four-wave mixing in an InGaAsP semiconductor laser," *IEEE Photon. Technol. Lett.*, vol. 3, pp. 1021–1023, 1991.

[4] M. C. Tatham, G. Sherlock, and L. D. Westbrook, "Compensation of fibre chromatic dispersion by optical phase conjugation in a semiconductor laser amplifier," *Electron. Lett.*, vol. 29, pp. 1851–1852, 1993.

[5] K. Inoue, "Four-wave mixing in an optical fibre in the zero-dispersion wavelength region," *J. Lightwave Technol.*, vol. 10, pp. 1553–1561, 1992.

[6] M. A. Summerfield, and R. S. Tucker, "Optimisation of frequency conversion by four-wave mixing in semiconductor optical amplifiers," *Optical Amplifiers and Their Applications*, paper FC4, pp. 110–114, 1996.

[7] J. P. R. Lacey, S. J. Madden, M. A. Summerfield, R. S. Tucker, and A.I. Faris, "Four-channel WDM optical phase conjugation using four-wave mixing in a single semiconductor optical amplifier," *Electron. Lett.*, vol. 31, pp. 743–744, 1995.

[8] J. Zhou, and K. J. Vahala, "Noise reduction in four-wave-mixing wavelength converters," *Conference on Lasers and Electro-Optics*, paper CThT1, p. 367, 1995.

[9] S. D. Personick, "Receiver design for digital fibre optic communication systems I," *Bell System Tech. Journal*, vol. 52, pp. 843–874, 1973.

[10] P. R. Morkel, and R. I. Laming, “Theoretical modeling of erbium-doped fiber amplifiers with excited-state absorption”, *Opt. Lett.*, vol. 14, pp. 1062–1064, 1989.

## FIGURE CAPTIONS

Figure 1. Experimental Setup. PC: polarisation controller, EDFA: erbium-doped fibre amplifier, PRBS: pseudo-random bit sequence, OSA: optical spectrum analyser.

Figure 2. Optical spectra: (a) input to both conjugators, (b) output of SOA based conjugator and (c) output of DSF based conjugator. (Resolution bandwidth = 0.05 nm).

Figure 3. Input and output conversion efficiencies.

Figure 4. Optical SNR of the conjugate wave. Circles and triangles represent experimental data with and without hole-burning grating respectively.

Figure 5. Conjugation noise figures of both conjugators with and without hole-burning grating. Circles and triangles represent experimental data with and without hole-burning grating respectively.

Figure 6. Eye penalty versus signal input power $P_{IN}$. Second order regression lines illustrate the trends.

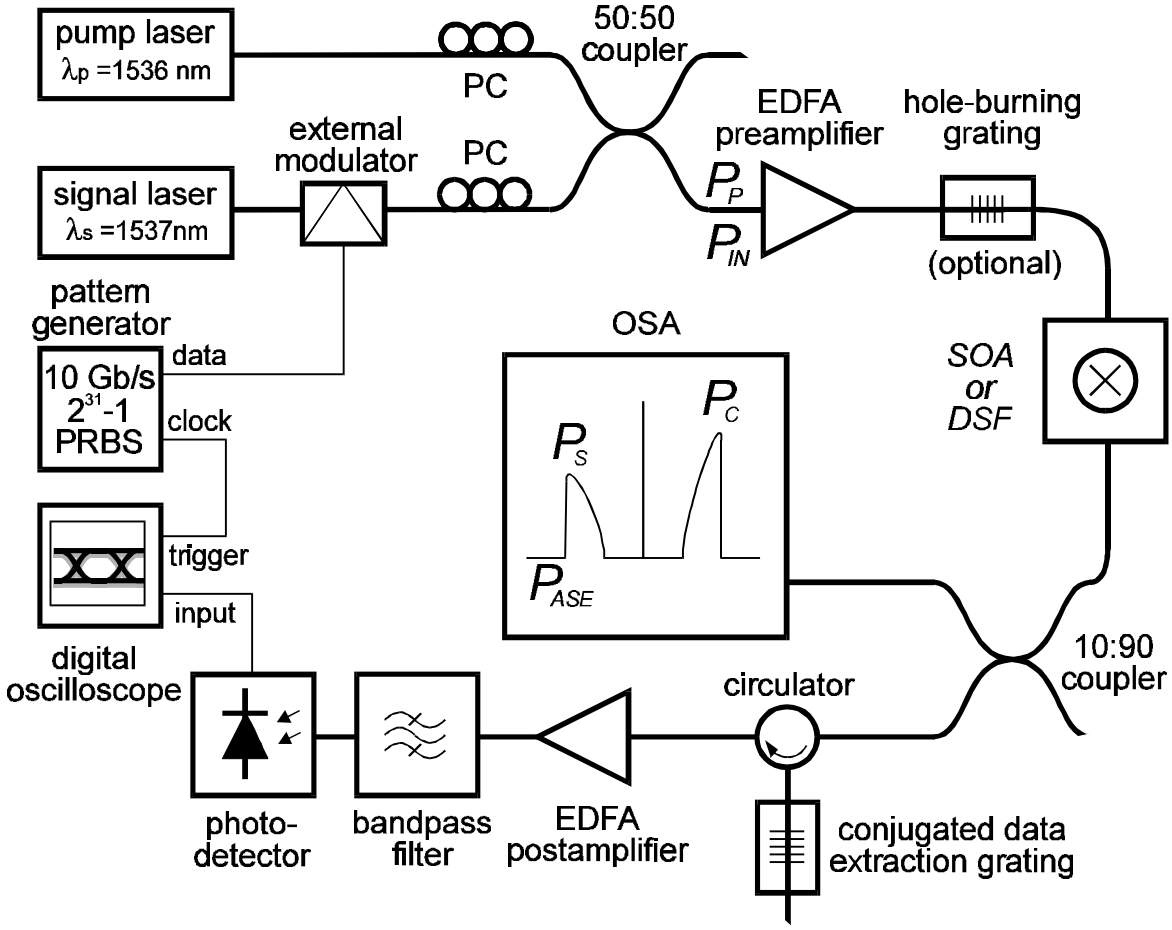


Figure 1. Experimental Setup. PC: polarisation controller, EDFA: erbium-doped fibre amplifier, PRBS: pseudo-random bit sequence, OSA: optical spectrum analyser.

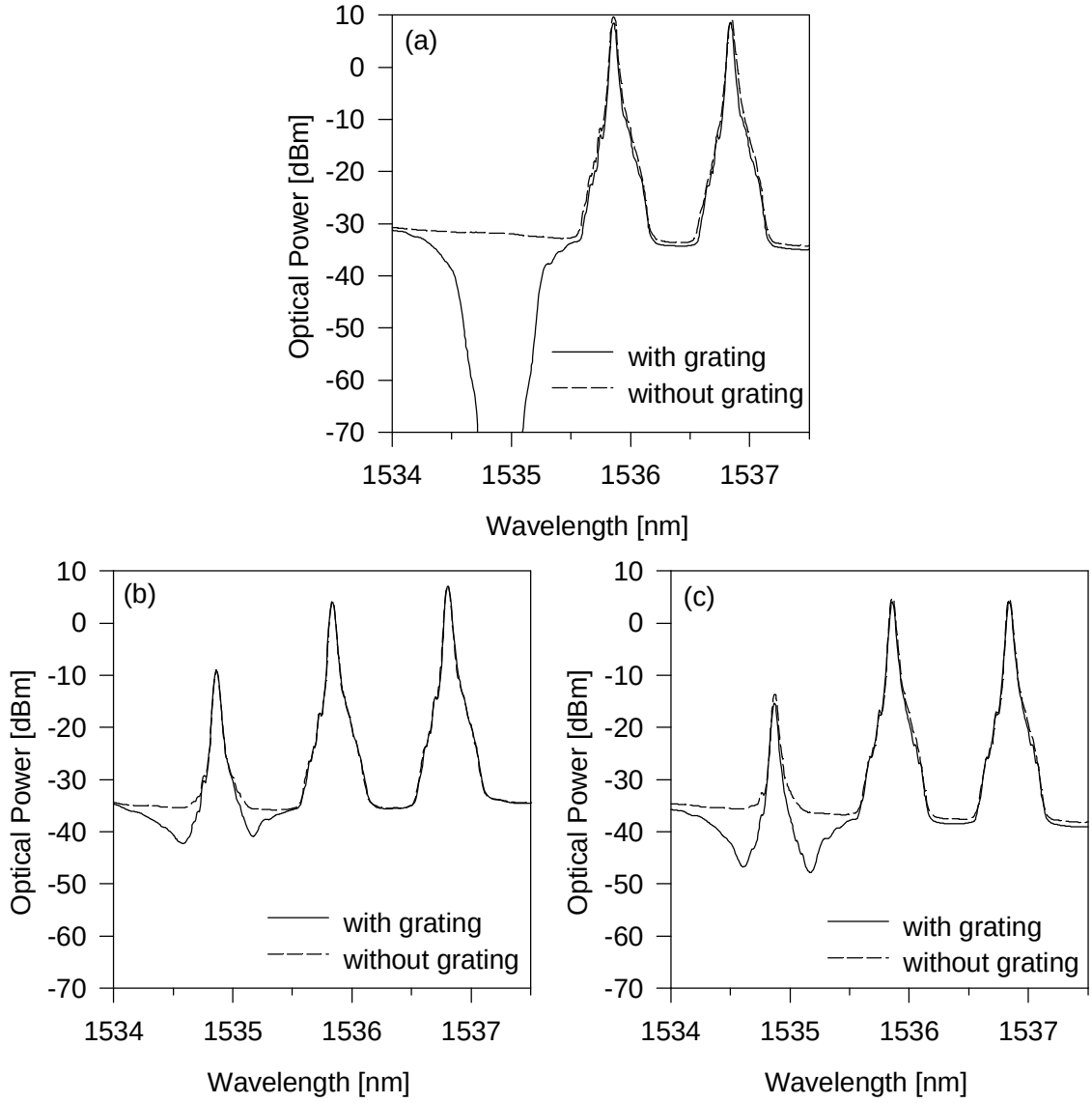


Figure 2. Optical spectra: (a) input to both conjugators, (b) output of SOA based conjugator and (c) output of DSF based conjugator. (Resolution bandwidth = 0.05 nm).

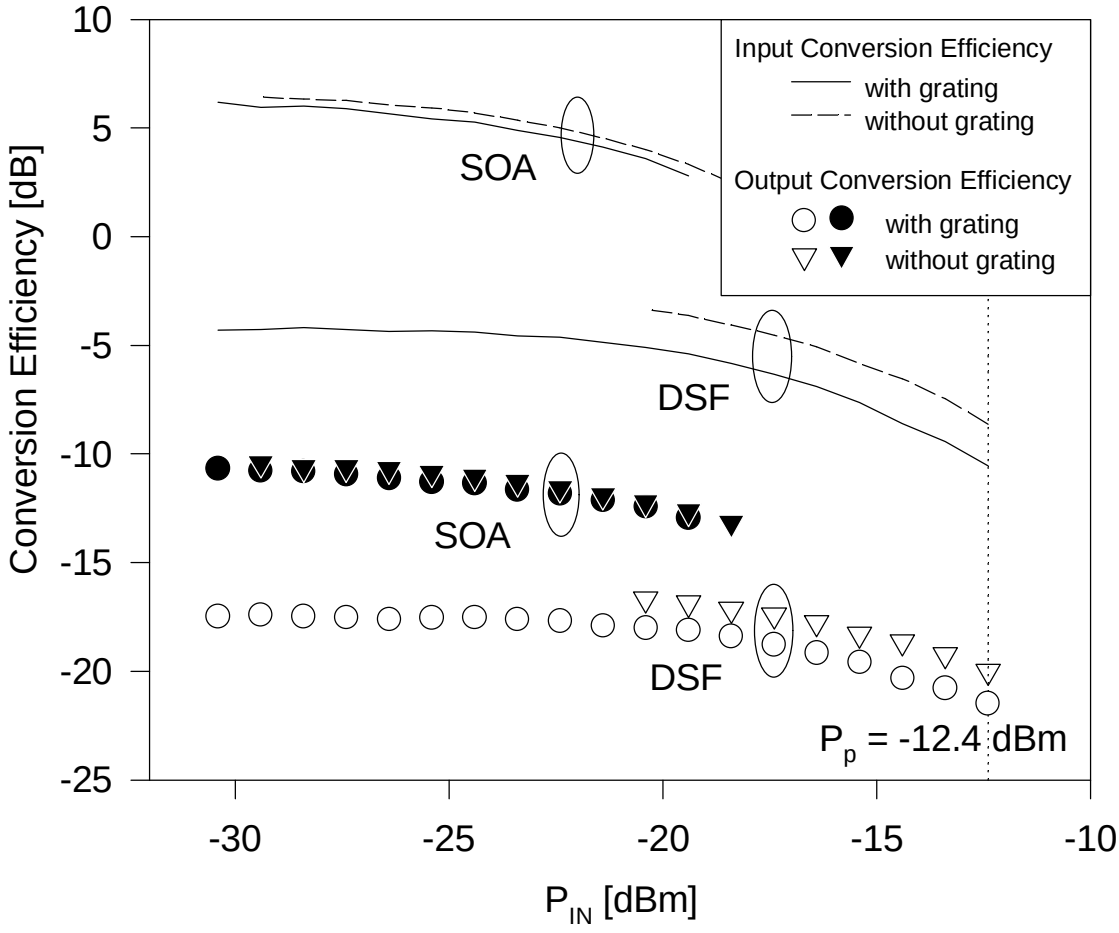


Figure 3. Input and output conversion efficiencies.

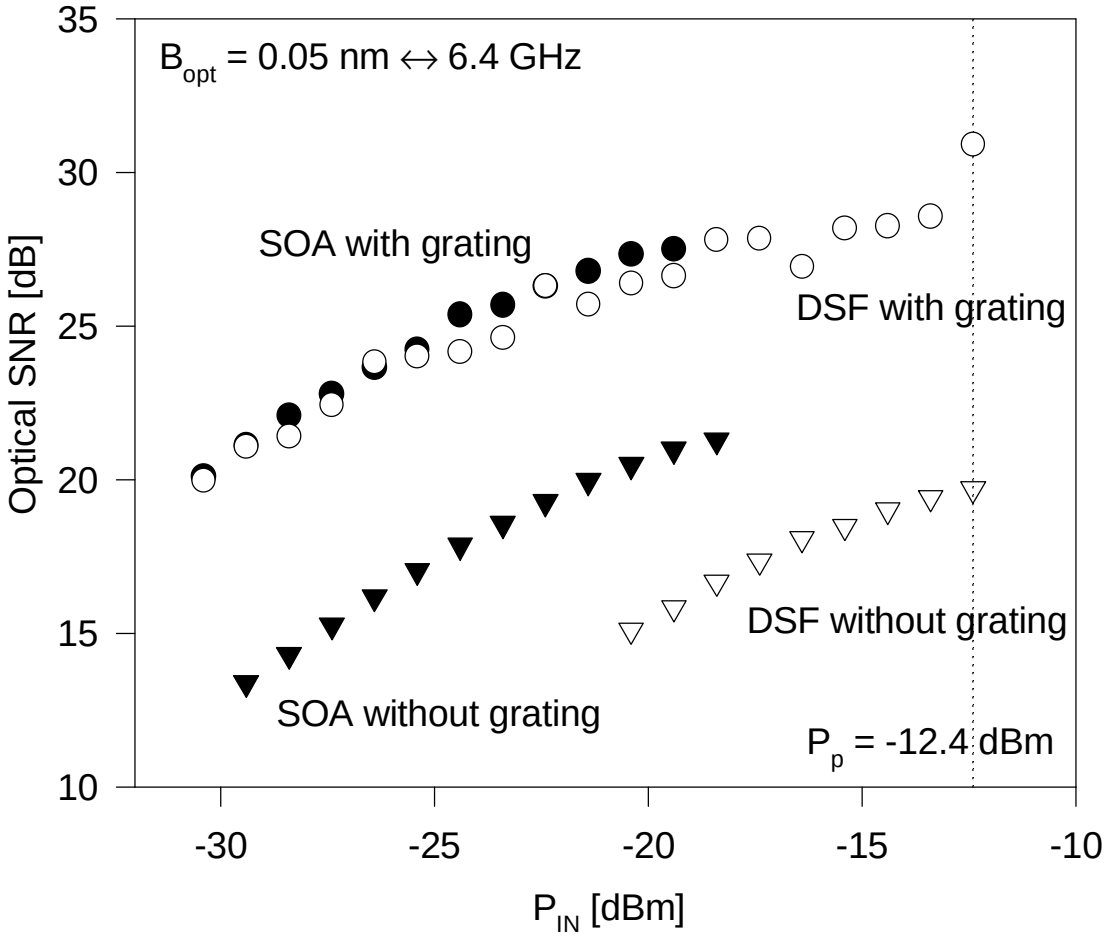


Figure 4. Optical SNR of the conjugate wave. Circles and triangles represent experimental data with and without hole-burning grating respectively.

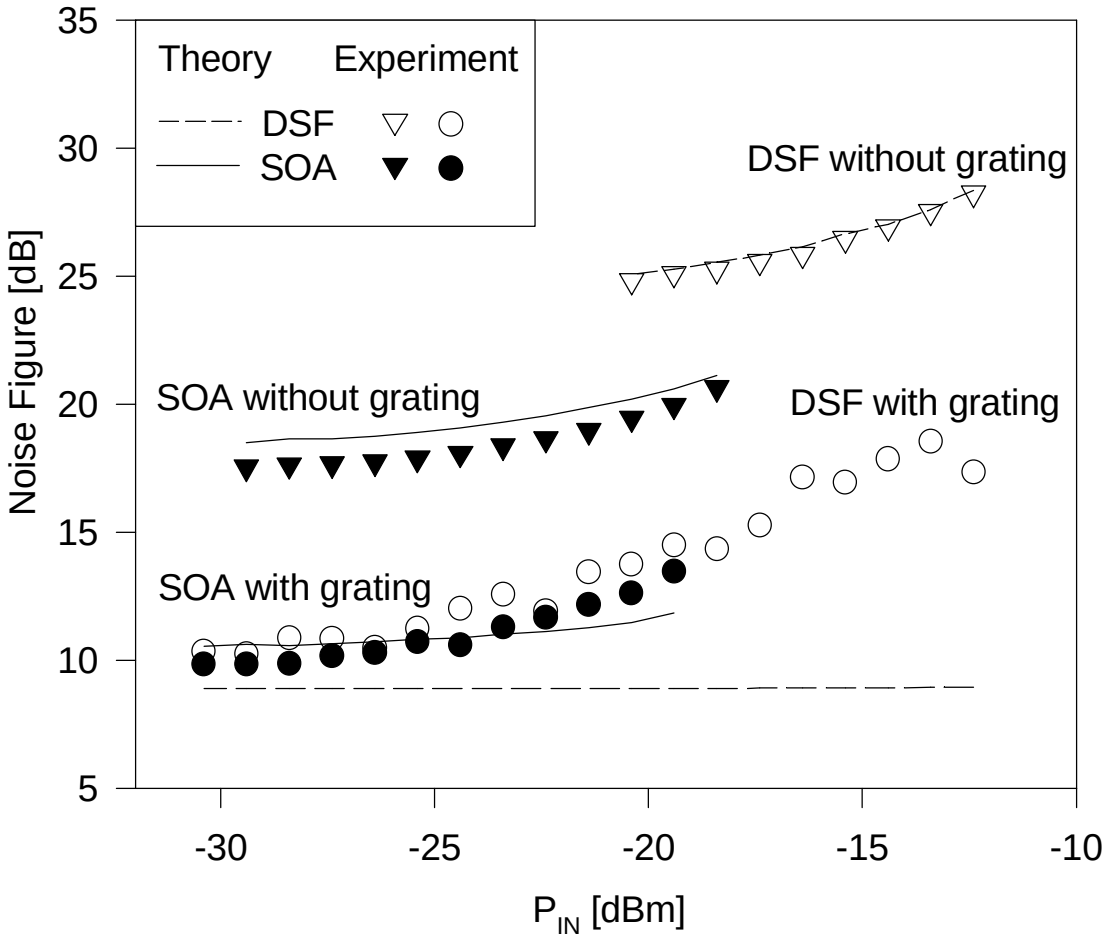


Figure 5. Conjugation noise figures of both conjugators with and without hole-burning grating. Circles and triangles represent experimental data with and without hole-burning grating respectively.

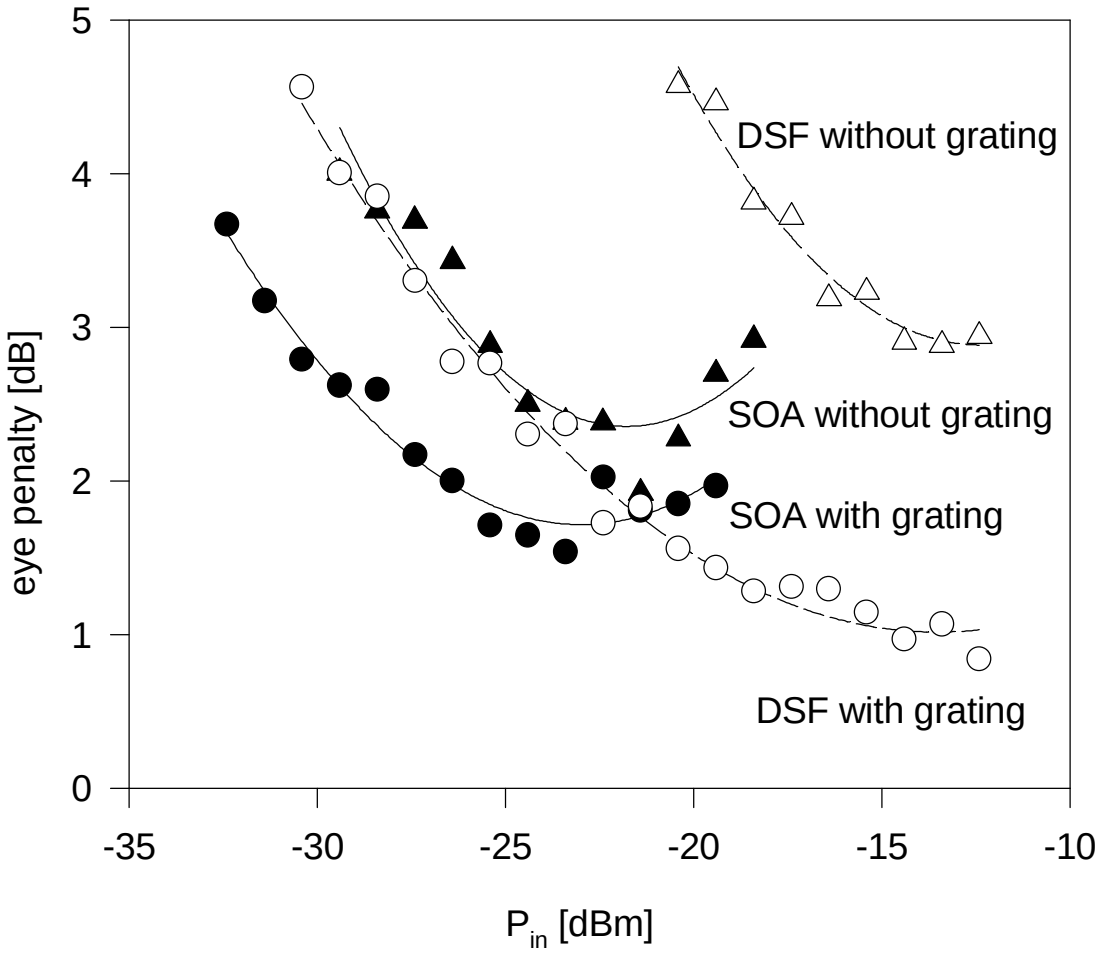


Figure 6. Eye penalty versus signal input power $P_{IN}$. Second order regression lines illustrate the trends.